Yield scalings of clusters with fewer than 100 nucleons

James B. Elliott* and Larry Phair*

*Nuclear Science Division, Lawrence Berkeley National Laboratory, Berkeley, California 94720

Abstract. This chapter gives a historical review of the scaling of yields of particles emitted from excited nuclei. The focus will be on what scaling is, what can be learned from scaling, the underlying theory of why one might expect particle yields to scale, how experimental particle yields have been observed to scale, model systems where particle (cluster) yields do scale and finally scaling observed in the particle yields of various low and medium energy nuclear reaction experiments. The chapter begins with a basic introduction to scaling in the study of critical phenomena and then reviews, in detail, Fisher's model which has all the aspects of scaling and can be directly applied to the counting of clusters, the most reliable measurement accessible to the experimental study of nuclear reaction. Next this chapter gives a history of the various scalings observed in nuclear reaction experiments and culminates with an estimate of the nuclear liquid-vapor phase boundary based upon measured particle yields.

Keywords: <Enter Keywords here>
PACS: 25.70.Pq, 05.70.Jk, 24.60.Ky, 64.60.Ak

INTRODUCTION

This chapter performs the modest task of covering seven decades worth of research on scaling in condensed matter and nuclear physics [1, 2, 3, 4, 5, 6, 7, 8, 9, 10, 11, 12, 13, 14, 15, 16, 17, 18, 19, 20, 21, 22, 23, 24, 25**?** , 27, 28, 29, 30, 31, 32, 33, 34, 35, 36, 37, 38, 39, 40, 41, 42, 43, 44, 45, 46, 47, 48, 49, 50, 51, 52, 53, 54, 55, 56, 57, 58, 59, 60, 61, 62, 63, 64, 65, 66, 67, 68, 69, 70, 71, 72, 73, 74, 75, 76, 77, 78, 79, 80, 81, 82, 83, 84, 85, 86, 87, 89, 88, 90, 91, 92, 93, 94, 95, 96, 97, 98, 99, 100, 101, 102, 103, 104, 105, 106, 107, 108, 109, 110, 111, 112, 113, 114, 115, 116, 117, 118, 119, 120, 121, 122, 123, 124, 125, 126, 127, 128, 129, 130, 131, 132, 133, 134, 135, 136, 137, 138, 139, 140, 141, 142, 143, 144, 145, 146, 147, 148, 149]. Inevitably, such and attempt will be incomplete and every reader will have his or her own favorite reference(s) omitted. To that end we humbly submit this chapter as a starting point for the motivated reader from which they can, perhaps, further their own understanding and research.

Scaling has been called "one of the three pillars of modern critical phenomena" [84]. The scaling hypothesis used in the study of critical phenomena was independently developed by several scientists, including Widom, Domb, Hunter, Kadanoff, Fisher, Patashinskii and Porkrovskii. See reference [8] for an authoritative review. The scaling hypothesis has two categories of predictions, both of which have been verified experimentally for a variety of physical systems.

The first category is a set of relations called *scaling laws*. These scaling laws relate the critical exponents α, β and γ which describe, for instance, the behavior of the the specific heat ($C \sim \varepsilon^{-\alpha}$), density differences of the phases ($\rho_l - \rho_v \sim \varepsilon^{\beta}$) and isothermal compressibility ($\kappa_T \sim \varepsilon^{-\gamma}$) for fluid systems; specific heat ($C \sim \varepsilon^{-\alpha}$), magnetization ($M \sim \varepsilon^{\beta}$) and isothermal susceptibility ($\chi_T \sim \varepsilon^{-\gamma}$)for magnetic systems or the singular part of the zeroth, first and second moment of the cluster distribution percolating systems near a critical point ($\varepsilon = (T_c - T)/T_c$ for physical systems and $(p_c - p)/p_c$ for percolating systems). In all the systems mentioned here, and more, these exponents are related via scaling law $\alpha + 2\beta + \gamma = 2$.

The second category is a sort of *data collapse*, which is best explained in terms of a the Ising model. We may write the equation of state as a functional relationship of the form $M = M(H, \varepsilon)$ where H is the applied magnetic field. Since $M(H, \varepsilon)$ is a function of two variable, it can be graphically represented as M vs ε for different H values. The scaling hypothesis predicts that all of these M vs ε curves can be "collapsed" onto a single curve provided that one plots not M vs ε but rather a scaled M (M divided by H to some power as a function of a scaled ε (ε divided by H to some other power). The predictions of the scaling hypothesis are supported by a wide range of experimental work with physical systems as well as computational models [3, 5, 6, 8, 16, 17, 19, 20, 22, 23, 28, 36, 43, 58, 69, 84, 101, 104, 106, 121, 125, 130, 131, 135, 147, 148]. Figure 1 shows some selected examples of data collapse.

The success of scaling in condensed matter is unquestionably impressive, but how is this sort of scaling related to the main topic of this chapter: the scaling of light fragment yields from nuclear multifragmentation experiments (where direct, straightforward measurements of standard thermodynamic quantities like density, pressure, chemical potential

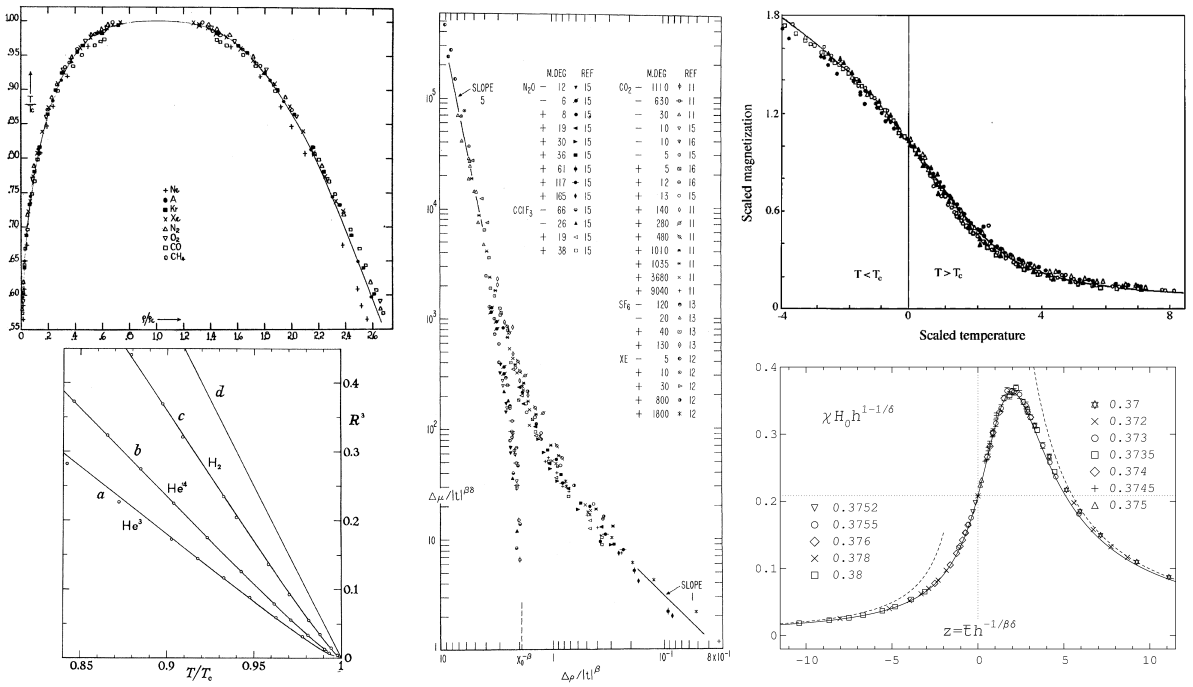

FIGURE 1. Examples of data collapse for various fluids and a magnetic system. Top left: the temperature T divided by the critical temperature T_c plotted as a function of the vapor density ρ_v and liquid density ρ_l normalized to the critical density ρ_c [3]. Bottom left: the cube of the normalized liquid vapor density difference $R = (\rho_l - \rho_v)/\rho_c = \Delta\rho/\rho_c$ plotted as a function of the normalized temperature T/T_c for "quantum" fluids (a: He^3, b: He^4 and c: H_2) and classical fluids (d), all fluids show scaling of the first category: $\rho_l - \rho_v \sim \varepsilon^\beta$ [5]. Center: the scaled chemical potential $|\Delta\mu|/|\varepsilon|^{\beta\delta}$ plotted as a function of the scaled density difference $|\Delta\rho|/|\varepsilon|^\beta$ in the critical region of several fluids (CO_2, Xe, SF_6, Ar, N_2O and $CClF_3$) [6]. Top right: scaled experimental *MHT* data on five different magnetic material: $CrBr_3$, EuO, Ni, YIG and Pd_3Fe [84]. Bottom right: the scaled susceptibility plotted as a function of the scaled temperature for the $d = 3$ Ising model [131].

and so on are impossible)? To see how the two are related we present a derivation of Fisher's model in the next section.

An aside: in the following text the more general term "cluster" will be used instead of "fragment" or "droplet." This is done to underscore the similarity between nuclear fragments and clusters (properly defined [21, 127]) in systems like the Ising model and droplets of fluid (classical or quantum). We also do this to avoid the unfortunate labeling of the process of nuclear cluster production as "fragmentation" which has a very specific meaning in condensed matter physics [41] that may be quite different that what the nuclear multifragmentation community has in mind.

FISHER'S MODEL AND SCALING

Physical cluster models

Fisher's model is an example of an equation of state that scales [7, 8, 104, 127] and is one of many physical cluster theories. Physical cluster theories of non-ideal fluids assume that the monomer-monomer interaction is exhausted by the formation of clusters and the clusters behave ideally and are independent of each other. Clusters of a given number of constituents A can be characterized by their mass m_A, a chemical potential per constituent μ and a partition function $q_A(T,V)$ that depends on the temperature T and volume V of the fluid. Because of the ideality of the fluid of clusters, the pressure and density are straightforward to determine the pressure p as

$$p = \frac{T}{V}\sum_{A=1}^{\infty} q_A(T,V)z^A \tag{1}$$

and the density ρ as

$$\rho = \frac{1}{V}\sum_{A=1}^{\infty} A q_A(T,V) z^A \tag{2}$$

where z is the fugacity $z = e^{\mu/T}$. The concentration of A clusters is then

$$n_A(T,z) = \frac{q_A(T,V)z^A}{V}. \tag{3}$$

Fisher's model

Fisher's contribution to physical cluster theory was to write the partition function of a cluster in terms of the free energy of the cluster. The energetic contribution to the free energy (very recognizable to nuclear scientists) is based on the liquid drop expansion

$$E_A = E_V + E_s \tag{4}$$

where E_V is the volume (or bulk) binding energy of the cluster which is taken to be $E_V = a_V A$ where a_V is the volume energy coefficient. The factor E_s is the energy loss due to the surface s (where surface is taken as the $d-1$ measure of a cluster that exists in d Euclidean dimensions) of the cluster. For clusters in d-dimensions this is usually taken to be $E_s = a_s A^{d-1/d}$. Because E_s is a measure of the volume energy loss due to the finiteness of the cluster, i.e. that the cluster has a surface, the surface energy coefficient is nearly equal to and opposite in sight to the volume energy coefficient: $a_s \simeq -a_V$. Fisher left the surface energy factor more general, writing $E_s = a_s A^{\sigma}$ where σ is some general exponent describing the ratio of the surface to the volume of the cluster.

Fisher estimated the entropic contribution to the free energy of the cluster based on a measure of the combinatorics of the number of clusters with surface s

$$g_s \simeq g_0 s^{-x} e^{b_s s} \tag{5}$$

where g_0 is some overall normalization, b_s can be thought of as the limiting entropy per unit surface of a cluster. This estimate can be tested by the study (and direct counting) of the number of self-avoiding polygons on the square lattice [89, 126, 137]. An example of a self-avoiding polygons on the square lattice is shown in Fig. 2. The study of self-avoiding polygons shows that to leading order $g_s \simeq 0.562301495 s^{-\frac{5}{2}} e^{0.97s}$ [89] while a fit to the direct counting of self-avoiding polygons (shown in Fig. 2) gives $0.62 s^{2.55} e^{0.97s}$ [126, 138]. Fisher then assumed that for large clusters, over some small temperature range the most probable or mean surface of a cluster would go as

$$\bar{s} \simeq a_0 A^{\sigma} \tag{6}$$

so that g_s could be re-written as

$$g_A \simeq g_0' A^{-\tau} e^{b_s' A^{\sigma}} \tag{7}$$

where $g_0' = g_0 a_0^{-x}$, $\tau = x\sigma$ and $b_s' = b_s a_0$. Which gives the entropy of a cluster as:

$$S_A = \ln g_A = \ln g_0' - \tau \ln A + b_s' A^{\sigma}. \tag{8}$$

The partition function of a cluster is then

$$\begin{aligned} q_A(T,V) &= V\left(\frac{2\pi m_A T}{h^2}\right)^{\frac{d}{2}} z^A \exp\left(-\frac{E_A - TS_A}{T}\right) \\ &= V g_0' A^{-\tau} \exp\left\{\frac{\left[\mu + a_V - \frac{d}{2A}T\ln\left(\frac{h^2}{2\pi m_A T}\right)\right]A}{T}\right\} \exp\left[-\frac{(a_s - Tb_s')A^{\sigma}}{T}\right]. \end{aligned} \tag{9}$$

Fisher identified the numerator of the first exponential as the distance from phase coexistence as measure by the chemical potential

$$\Delta\mu = \mu + a_V - \frac{d}{2A}T\ln\left(\frac{h^2}{2\pi m_A T}\right), \tag{10}$$

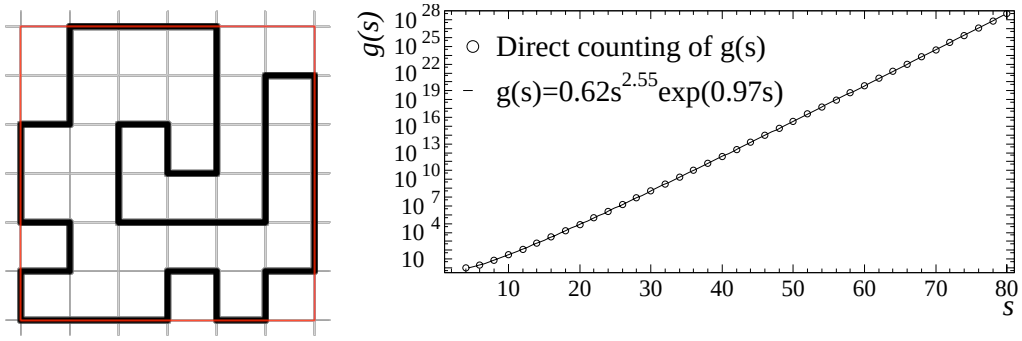

FIGURE 2. Left: an example of a self-avoiding polygon on the square lattice with $A = 23$ and $s = 40$, there are $49,157,726,494$ ways to form a cluster with this number and surface. Right: a fit using Eq. (5) (solid line) to the direct counting of g_s (open circles).

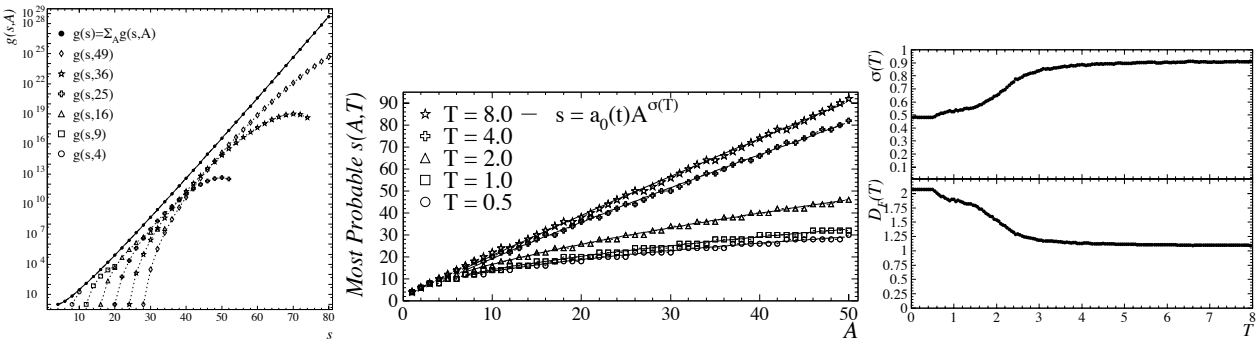

FIGURE 3. Left: the direct counting of g_s (open circles) and $g_{s,A}$ (symbols). Middle: the most probable surface as a function of A and T. Right: top: the effective surface to volume exponent σ as a function of temperature; bottom: the fractal dimension D_F as a function of temperature, see references [36, 138] for details.

at coexistence (or condensation) $\Delta\mu = 0$ and $\mu_{\text{coex}} = \frac{d}{2A} T \ln\left(\frac{h^2}{2\pi m_A T}\right) - a_v$. The "microscopic" part of the surface tension $(a_s - T b'_s)$ vanishes at the critical point, leaving only a power law (which has been explicitly verified in computational systems [13, 20, 39, 36, 40, 48, 51, 55, 59, 65, 67, 68, 69, 70, 82, 85, 86, 93, 101, 104, 130, 135, 138, 147] and implicitly verified in a wide variety of physical fluids [9, 12]). Thus

$$T_c = \frac{a_s}{b'_s}. \tag{11}$$

Using Eq. (10) and assuming little or no temperature dependence of a_s and b'_s over the temperature range in question, then we may re-write Eq. (9) as

$$q_A(T,V) = V g'_0 A^{-\tau} \exp\left(\frac{\Delta\mu A}{T}\right) \exp\left(-\frac{a_s \varepsilon A^\sigma}{T}\right) \tag{12}$$

which gives the familiar expression for the cluster number concentration

$$n_A(T) = g'_0 A^{-\tau} \exp\left(\frac{\Delta\mu A}{T}\right) \exp\left(-\frac{a_s \varepsilon A^\sigma}{T}\right). \tag{13}$$

Caveats

Before proceeding further, we wish to test Fisher's assumptions on the most probable or mean surface $\bar{s}$ of a cluster. We may do this by using the combinatorics of self-avoiding polygons and noting that, at phase coexistence, Eq. (14)

is the product of the combinatorial factor and a Boltzmann factor that depends on the surface energy:

$$n_{s,A}(T) \propto g_{s,A} \exp\left(-\frac{a_s s}{T}\right) \tag{14}$$

where now we write things explicitly in terms of both cluster number A and cluster surface s [136, 138]. The mean surface of a cluster is then just

$$\bar{s} = \frac{\sum_{A=1}^{\infty} s n_{s,A}(T)}{\sum_{A=1}^{\infty} n_{s,A}(T)}. \tag{15}$$

Using the direct counting of $g_{s,A}$ (see Fig. 3) and setting (as in the Ising model) $a_s = 2$ (thus $T_c \simeq \frac{2}{0.97} = 2.06$) we can determine the most probable surface of a cluster of A constituents at temperature T. Fitting $\bar{s}(A)$ with $a_0 A^{\sigma}$ letting a_0 and σ be free parameters we can study Fisher's assumption. Figure 3 shows that at low temperatures $\sigma \simeq 0.5$ as one would expect for a $d = 2$ system. As the temperature increases the value of σ increases. At $T = T_c \simeq 2.06$, $\sigma \simeq 0.65$, a change of 30% from the $T = 0$ value of σ. Thus, Fisher's implicit assumption that σ is a constant is only good to the 30% level in this example. Looking at the accpeted values of $\sigma = 8/15$ from the $d = 2$ Ising model [147] and comparing it to the expected $T = 0$ value of $\sigma = 1/2$ shows this assumption to be good to the 6.67% level for $0 \leq T \leq T_c$. Looking at the accpeted values of $\sigma = 0.63946 \pm 0.0008$ from the $d = 3$ Ising model [135] and comparing it to the expected $T = 0$ value of $\sigma = 2/3$ shows this assumption to be good to the 4.08% level for $0 \leq T \leq T_c$. When the temperature is restricted to a very small range around $T \sim T_c$ this assumption is quite good.

Another possible problem with this assumption is not only the dependence of σ on temperature, but the dependence of a_0 on temperature and cluster size A. Fisher implicitly assumed that for $A \to \infty$ a_0 is some constant. Using Eq. (15) with the $g_{s,A}$ of self-avoiding polygons we can test this assumption, by examining

$$a_0 = A^{-\sigma} \bar{s} = A^{-\sigma} \frac{\sum_{A=1}^{\infty} s n_{s,A}(T)}{\sum_{A=1}^{\infty} n_{s,A}(T)}. \tag{16}$$

In this example $\sigma = 8/15$ is taken from the $d = 2$ Ising model and $T = 1 \simeq T_c/2$. Figure 4 shows the results. For $A < 10$ the value of a_0 clearly shows "shell effects" that cause fluctuations on the order of 10% of the limiting value of a_0. For $A \geq 10$ the shell effects diminish and the limiting value of $a_0 \simeq 4.6$ is reached. Thus in this example Fisher's assumption holds for $A \geq 10$ [136].

Figure 4 also shows the results from a direct counting of $d = 3$ self-avoiding polyhedra [140] and clusters from the $d = 3$ simple cubic Ising lattice [148]. The $g_{s,A}$ for the self-avoiding polyhedra has been directly counted up to $A = 9$, counting for $A \geq 10$ is prohibitively time consuming on today's computers. However, the dependence of a_0 on cluster size and temperature can be investigated just as in the case of the $d = 2$ polygons (using $\sigma = 0.63946 \pm 0.0008$ and $a_s = 2$, which holds for the $d = 3$ Ising model as well). We see that for the lowest temperature ($T = 1$, as compared to the $d = 3$ Ising model $T_c = 4.51152 \pm 0.00004$ [135]) the shell effects are evident: for perfect cubes $A = 1$ and $A = 9$ $a_0 = 6$ as expected. As the temperature increases the shell effects are washed out and a_0 shows a steady rise with A. The steady rise of a_0 with A could indicate that $\sigma \geq 0.63946 \pm 0.0008$ (which violates the first category of scaling as will be seen below) or that the limiting behavior Fisher assumed does not set in until $A \gg 50$. In either case, it seems this assumption is poorer in $d = 2$ than in $d = 3$.

Finally, we note that Fisher's model is valid only for $T \leq T_c$: temperatures greater than T_c yield cluster surface free energies that are negative, and thus unphysical. The parametrization used in Fisher's model this is only one example of a more general form of the scaling assumption $n_A = A^{-\tau} f(X)$ and $X = A^{\sigma} \varepsilon^{\phi}$ and where $f(X)$ is some general scaling function which [20, 22, 28]:

- is valid on both sides of the critical point;
- for small X ($T \sim T_c$ and small A) and $\varepsilon > 0$, $f(X)$ will vary as $\exp(-X)$ with $\sigma = 1/(\beta\delta) = 1/(\gamma+\beta) \sim 0.64$ for three dimensional Ising systems, $8/15$ for two dimensional Ising systems or ~ 0.45 for three dimensional percolation systems and $\phi = 1$;
- for large X (T far from T_c or large A) and $\varepsilon > 0$, $f(X)$ will vary as $\exp(-X)$ with $\sigma = (d-1)/d$ for all d dimensional systems and with $\phi = 2\nu$, where $\nu \sim 0.63$ for three dimensional Ising systems, $\nu = 1$ for two dimensional Ising systems and $\nu \sim 0.88$ for three dimensional percolation lattices.

Figure 5 shows the general form of the scaling function $f(X)$ for percolation systems [20, 22]. However, this more general scaling function $f(X)$ does not lend itself as easily to a physical interpretation as does the parameterization

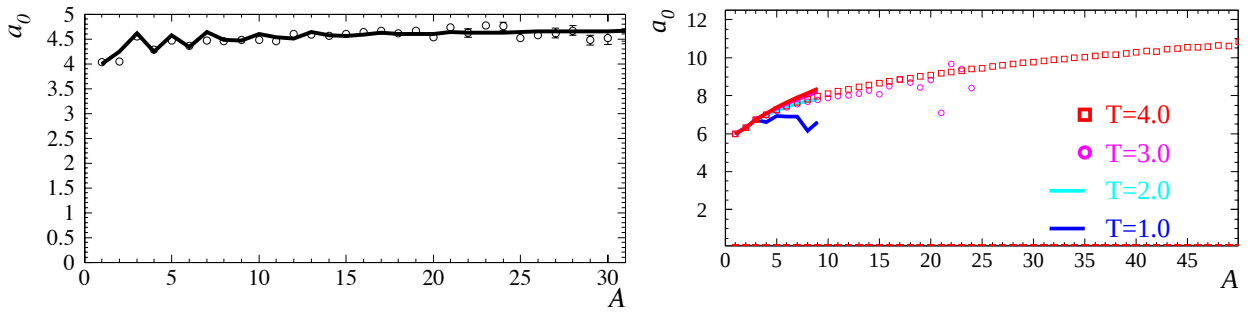

FIGURE 4. Left: the geometrical pre-factor for the mean surface to cluster size relation a_0 as a function of cluster size A. The solid line shows the results for Eq. (16), open circles show a_0 for $d = 2$ Ising clusters [136]. Right: top: the effective surface to volume exponent σ as a function of temperature; bottom: the fractal dimension D_F as a function of temperature, see reference [140] for details.

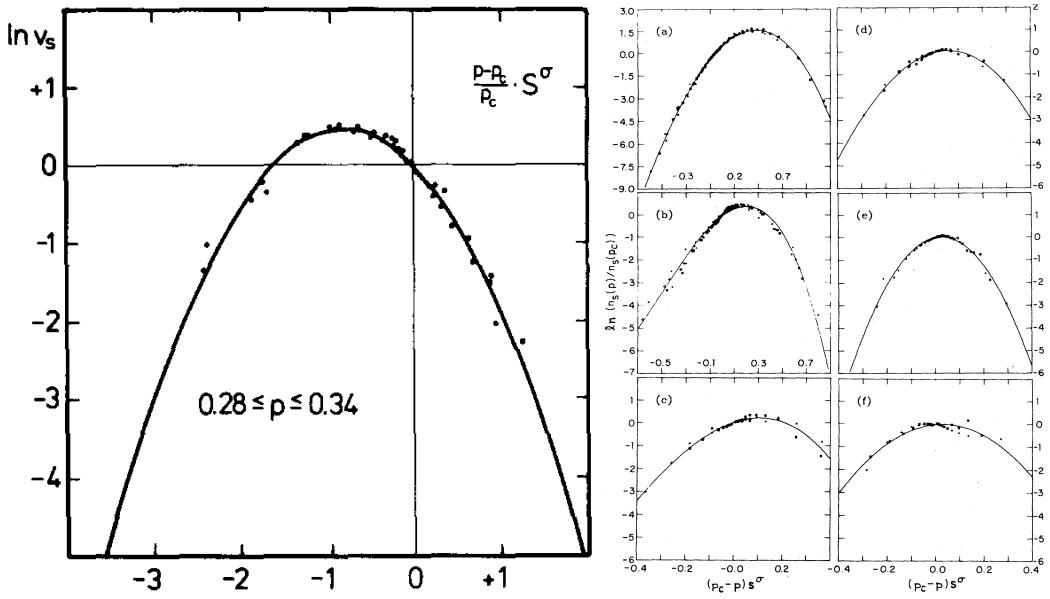

FIGURE 5. Left: the scaled cluster yields $v_S = n_A(p)/A^{-\tau}$ as a function of the argument of the scaling function $X = A^\sigma(p - p_c)/p_c$ for bond building (p is the bond building probability) $d = 3$ percolation on a square lattice with 10^6 sites. Data from different p follow the same curve as required by the scaling hypothesis. The parabola is the general form of $f(X)$ [20]. Right: the natural log of the scaled cluster yields as a function of $p_c X$ (solid points) for (a) $d = 2$ to (f) $d = 7$ together with the least-squares fits (solid lines) [22].

given by Fisher's model and it is this physical interpretation which is important to the application of this method to the nuclear data.

With these caveats in mind we can proceed, cautiously, and see how both categories of scaling arise in Fisher's model.

Scaling from Fisher's model

Starting with the second category of scaling first, namely: data collapse. We start by looking at the cluster concentrations in Fisher's model given by Eq. (13). Dividing both sides by the power law factor and the chemical potential

factor then gives:

$$\frac{n_A(T)}{g_0' A^{-\tau} \exp\left(\frac{\Delta\mu A}{T}\right)} = \exp\left(-\frac{a_s \varepsilon A^\sigma}{T}\right). \tag{17}$$

This shows that scaling the cluster concentrations by the power law and chemical potential factors against the cluster surface free energy should collapse the data for each cluster size A at each temperature T to a single curve. Figure 6 shows this type of scaling and data collapse in percolation [136] and Ising model cluster yields [135]

To arrive at the first category of scaling from Fisher's model, we combine the general equations for pressure and density for physical cluster models, equations (1) and (2), with Fisher's estimate of the cluster partition function, Eq. (12) giving

$$p = T \sum_{A=1}^{\infty} g_0' A^{-\tau} \exp\left(\frac{\Delta\mu A}{T}\right) \exp\left(-\frac{a_s \varepsilon A^\sigma}{T}\right) \text{ and } \rho = \sum_{A=1}^{\infty} g_0' A^{1-\tau} \exp\left(\frac{\Delta\mu A}{T}\right) \exp\left(-\frac{a_s \varepsilon A^\sigma}{T}\right). \tag{18}$$

Along the coexistence line, i.e. $\Delta\mu = 0$, we have

$$p_{\text{coex}} = T \sum_{A=1}^{\infty} g_0' A^{-\tau} \exp\left(-\frac{a_s \varepsilon A^\sigma}{T}\right) \text{ and } \rho_{\text{coex}} = \sum_{A=1}^{\infty} g_0' A^{1-\tau} \exp\left(-\frac{a_s \varepsilon A^\sigma}{T}\right). \tag{19}$$

At the critical point we have

$$p_c = T_c \sum_{A=1}^{\infty} g_0' A^{-\tau} \text{ and } \rho_c = \sum_{A=1}^{\infty} g_0' A^{1-\tau}. \tag{20}$$

Taking the ratios of equations (19) to (20) gives the reduced pressure p_{coex}/p_c and reduced density $\rho_{\text{coex}}/\rho_c$

$$\frac{p_{\text{coex}}}{p_c} = \frac{T \sum_{A=1}^{\infty} A^{-\tau} \exp\left(-\frac{a_s \varepsilon A^\sigma}{T}\right)}{T_c \sum_{A=1}^{\infty} A^{-\tau}} \text{ and } \frac{\rho_{\text{coex}}}{\rho_c} = \frac{\sum_{A=1}^{\infty} A^{1-\tau} \exp\left(-\frac{a_s \varepsilon A^\sigma}{T}\right)}{T_c \sum_{A=1}^{\infty} A^{1-\tau}} \tag{21}$$

which has the advantage of being free of the constant g_0'. In order to further test the results above, we determine the magnetization M of the $d = 3$ Ising model using Eq. (21) and recalling that the magnetization per lattice site is simply:

$$M = 1 - \frac{\rho}{\rho_c}. \tag{22}$$

Using the values of σ, τ, c_0 and T_c determined from fitting clusters on the $d = 3$ Ising lattice shown in Fig. 6 [135] in Eq. (21), Eq. (22) gives one branch of the magnetization curve, the branch for $M > 0$. Since the magnetization is symmetric about the origin, the points for $M < 0$ are reflections of the points for $M > 0$. The results are shown as the open circles in the bottom right plot of Fig. 6. These results compare well with a parametrization for $M(T)$ [135] (used as a "benchmark") shown as a solid line in the bottom right plot of Fig. 6. Better agreement with the $M(T)$ parameterization is found when the values of $\sigma = 0.63946 \pm 0.0008$, $\tau = 2.209 \pm 0.006$ (from the scaling relations in Fisher's model developed below and values of $\beta = 0.32653 \pm 0.00010$ and $\gamma = 1.2373 \pm 0.002$ [135]), $a_s = 12$ and $T_c = 4.51152 \pm 0.00004$ were used. Nearly perfect results were observed when a_s was "tuned" to 16 and the more precise value of T_c and the scaling relation exponent values were used. The agreement between the magnetization values calculated via the sum in Eq. (22) and the $M(T)$ parameterization for $0 < T < T_c$ suggest that the ideal gas assumptions in Fisher's model allow for an accurate description of the system even up to densities as high as ρ_c.

By combining equations (19) and (20) we can arrive at the scaling relations as follows:

$$\frac{\rho_c - \rho_{\text{coex}}}{\rho_c} = \frac{g_0'}{\rho_c} \sum_{A=1}^{\infty} A^{1-\tau} \left[1 - \exp\left(-\frac{a_s \varepsilon A^\sigma}{T}\right)\right] \simeq \frac{g_0'}{\rho_c \sigma} \Gamma\left(-\frac{\tau-2}{\sigma}\right) \left(\frac{a_s}{T_c}\right)^{\frac{\tau-2}{\sigma}} \varepsilon^{\frac{\tau-2}{\sigma}} = B\varepsilon^\beta \tag{23}$$

since as $T \to T_c$ large values of A give the dominant contribution to the above sum and the sum may be replaced by an integral [18]. Here $\beta = \frac{\tau-2}{\sigma}$. This leads directly to the familiar $\rho_l - \rho_v \sim \varepsilon^\beta$ relation.

Similarly, one finds that along the coexistence line the specific heat at constant volume is [7, 127]

$$C_V = T^2 \left.\frac{\partial^2 \frac{p_{\text{coex}} V}{T}}{\partial T^2}\right|_V \sim \varepsilon^{\frac{1-\tau}{\sigma}} \sim \varepsilon^{-\alpha} \tag{24}$$

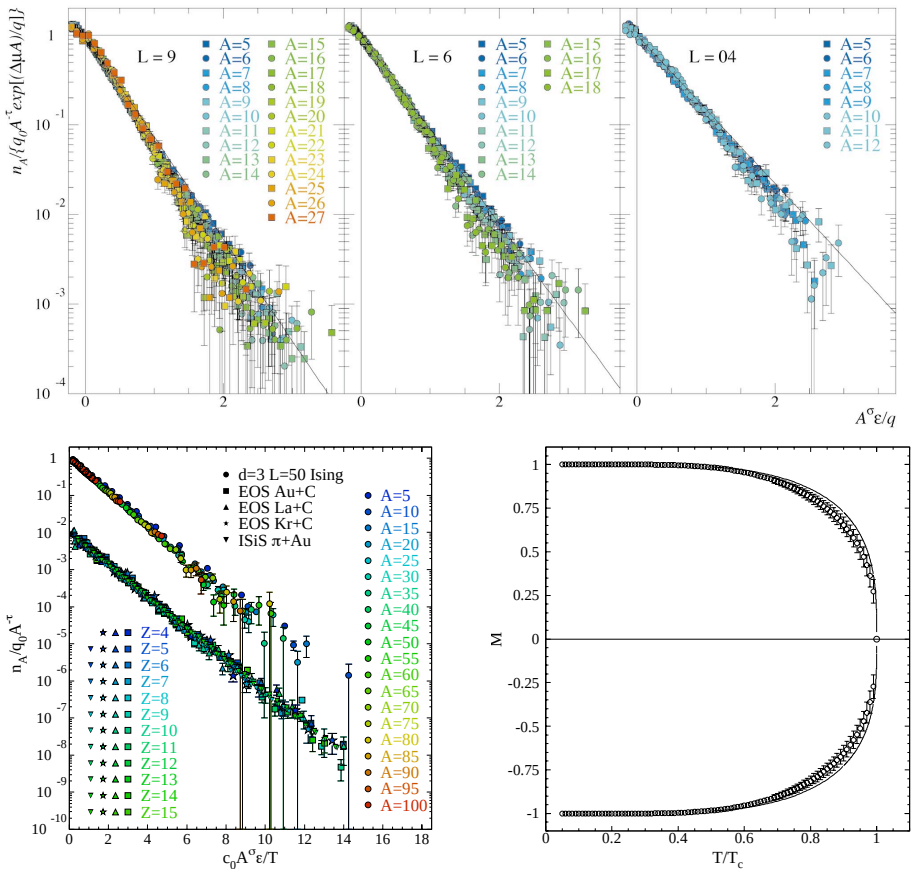

FIGURE 6. Top three plots: the scaling of Eq. (17) for $d = 3$ bond breaking percolation on the simple cubic lattice of side $L = 9$, 6 and 4 (q is the bond breaking probability) [130]. Bottom left plot: the scaling of Eq. (17) for $d = 3$ Ising model on the simple cubic lattice of side $L = 50$ [135]. Bottom right plot: the magnetization as a function of reduced temperature. The open circles show the magentization predicted via Fisher's model (see text) and the solid line shows a parameterization for the magnetization.

thus $\alpha = \frac{\tau-1}{\sigma}$.

Finally, one the isothermal compressibility can be found to be [104]

$$\kappa_T = \frac{1}{\rho}\frac{\partial \rho}{\partial p}\bigg|_T \sim \varepsilon^{\frac{\tau-3}{\sigma}} \sim \varepsilon^{-\gamma} \tag{25}$$

thus $\gamma = \frac{3-\tau}{\sigma}$.

The three examples above show how Fisher's model leads to the power laws that describe the behavior of a system near its critical point. Putting the equations defining α, β and γ together recovers the scaling law $\alpha + 2\beta + \gamma = 2$ and illustrates that (aside from so-called "hyperscaling") there are only two independent exponents (σ and τ in Fisher's model) from which all others are recovered.

Excluded volume effects on Fisher's model

The final entry into this section discussing Fisher's model is the effect of the finite volume of real, physical clusters. Fisher's model, like any physical cluster model, assumes that the clusters have no volume. Obviously this is not the case, so how well does Fisher's model do in describing real clusters which have some finite volume? We have already seen in Fig. 6 that Fisher's model collapses the cluster concentrations of computer models quite well when the parameters (exponents, critical temperature, surface energy coefficient) are allowed to vary; the values returned for these parameters from the fitting procedures usually agree well with expected values [130, 135] (with the exception of

σ for the $d=3$ Ising model, though that discrepancy may be the result of using clusters that are too small, see Fig. 4 and discussion above).

In the case of physical fluids the effects of the finite volume of clusters at the critical point can be studied by realizing that Fisher's model gives the compressibility factor as the ratio of two Riemann ζ functions

$$\frac{p_c}{T_c\rho_c}=\frac{\sum_{A=1}^{\infty}A^{-\tau}}{\sum_{A=1}^{\infty}A^{1-\tau}}=\frac{\zeta(\tau)}{\zeta(\tau-1)}. \tag{26}$$

When the compressibility factor for real fluids (e.g. He^4, Ne, ethane, acetylene, CH_3CH, C_2H_5Cl, etc.) was analyzed it was found that $\tau=2.202\pm0.004$ which is to be expected for $d=3$ systems [9]. This result indicates that for real fluids the value of τ is not greatly affected by the finite size of the clusters. An analysis of the "excluded-volume" effect and Fisher's model later showed that the scaling laws (e.g. $\alpha+2\beta+\gamma=2$) were unchanged [11].

If the exponents and scaling laws are unaffected by the finite volume of clusters, then what are the effects of the finite volume of the clusters? To answer this question we turn our attention back to the self-avoiding polygons [137]. Figure 4 shows that using the directly counted combinatorics $g_{s,A}$ we were able to reproduce the behavior of clusters from the $d=2$ Ising model on a square lattice, up to a point. The critical temperature predicted by the self-avoiding polygons $T_c=2.06$ is approximately 10% below Onsager's analytically determined value $T_c=2.26915\ldots$.

To improve the above estimate of T_c, at coexistence, we think of an initial configuration of a cluster with $A_0\to\infty$ constituents and surface s_0 and a final state of a cluster of A constituents and surface s and its complement: a cluster of $A_c=A_0-A$ constituents and surface s_c. This assumes stochastic cluster formation and is supported by the Ising cluster's Poissonian nature [135]. Now the free energy of cluster formation is

$$\Delta G=\Delta E-T\Delta S+p_{\rm coex}\Delta V=a_V\left[A+(A_0-A)-A_0\right]+a_s(s+s_c-s_0)-T\left(\ln g_{s,A}+\ln g_{s_c,A_c}-\ln g_{s_0,A_0}\right)+p\Delta V \tag{27}$$

ΔV is the volume change between the initial and final configurations. All terms $\propto A$ cancel. In the limit $A_0\to\infty$, $s_c\approx s_0$ and $\ln g_{s_c}\approx\ln g_{s_0}$ leaving only the cluster's contribution to the ΔG. The volume change for the lattice gas is

$$\Delta V=a_1\left[A+(A_0-A)-A_0\right]+l(s+s_c-s_0) \tag{28}$$

where a_1 is the geomertrical prefactor relating the cluster volume to the cluster number A and l is the interaction range between two constituents, one spacing on a lattice: $l=1$. The second term of Eq. (28) arises from the fact that no two clusters can come within a distance l of each other and be considered two clusters, thus each cluster has a volume ls surrounding it which is excluded to all other clusters.

In in the $A_0\to\infty$ limit the first term of Eq. (28) cancels. The second term of Eq. (28) depends only on the cluster's surface. Writing the partition function for a cluster as $q_s(V,T)\sim\exp(-\Delta G/T)$ [18] and now including the excluded volume factor from Eq. (28) gives

$$n_s(T)\sim g_s\exp\left(-\frac{a_s s}{T}\right)\exp\left(\frac{2p_{\rm coex}ls}{T}\right)\sim g_0 s^{-x}\exp\left[-\frac{s(a_s-Tb_s+2p_{\rm coex}l)}{T}\right]. \tag{29}$$

The factor of two arises from moving the cluster from one phase to the other: imagine taking a cluster from the condensed phase, which leaves behind a bubble, and placing it in dilute phase. Both the bubble in the condensed phase and the cluster in the dilute phase have the associated excluded volume contribution of ls.

Just as above, the "microscopic" portion of the surface free energy vanishes at the critical point so

$$T_c=\frac{a_s+2p_cl}{b_s}=\frac{a_s}{b_s}+\frac{2p_cl}{b_s}. \tag{30}$$

The first term in Eq. (30) can be thought of as the "ideal" critical temperature and the second term can be thought of as the correction that arises due to the finite volume of the cluster. Working at the critical point with $p_c\approx0.11$ for the $d=2$ Ising model, Eq. (30) gives $T_c=2.29$, within 1% of the Onsager value.

Equation (29) also provides a good description of Ising cluster yields. Figure 7 shows the Ising yields ($n_A(T)=\sum_s n_{s,A}(T)$) of a two dimensional square lattice of side $L=80$ and the predictions of Eq. (13) and (29) (both at coexistence and both using the directly counted $g_{s,A}$ combinatorics of the self-avoiding polygons) with *no fit parameters*.

Figure 7 also shows the integrated quantities of the density and pressure along the coexistence line for the $d=2$ Ising system. The values of $\rho_{\rm coex}$ and $p_{\rm coex}$ determined from calculations on the square lattice [148] (open circles),

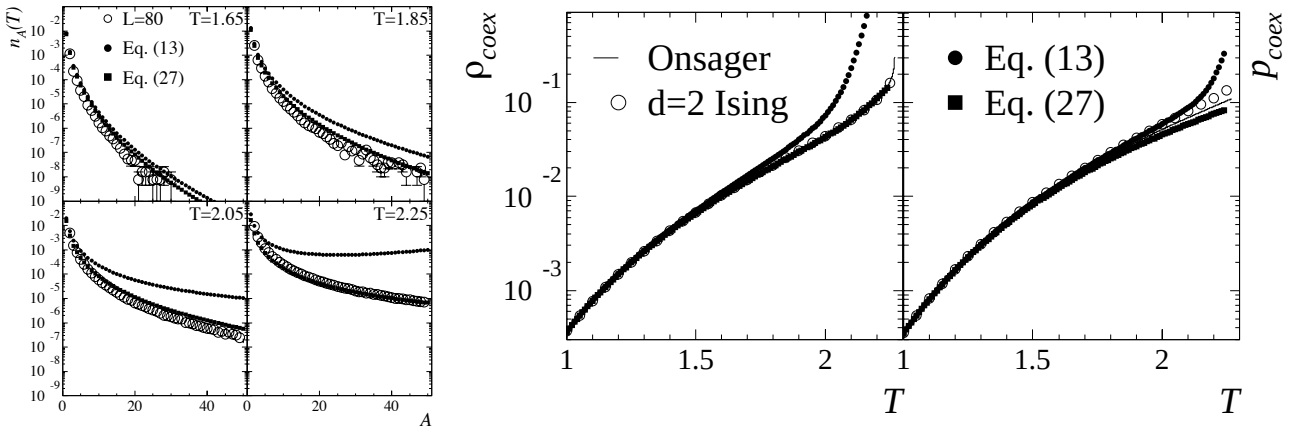

FIGURE 7. Left: Ising cluster yields from the $d = 2$ square lattice (open circles) at four different temperatures compared to Eq. (13) (filled circles) and (29) (filled squares) (both at coexistence and both using the directly counted $g_{s,A}$ combinatorics of the self-avoiding polygons) with *no fit parameters* [137]. Right: the density $\rho_{\rm coex}$ and pressure $p_{\rm coex}$ at coexistence from the Onsanger solution (solid line), from $d = 2$ Ising calculations on the square lattice [148] (open circles), from Eqs. (19) and (13) (filled circles) and from Eqs. (19) and (29) (filled squares).

from Eqs. (19) and (13) (filled circles) and from Eqs. (19) and (29) (filled squares) are compared to the analytical solution of Onsager (solid line). To calculate the pressure and density from the self-avoiding polygon combinatorics and the finite cluster volume concentration, the equations

$$p_{\rm coex} = T\sum_{s,A} g_{s,A}\exp\left[-\frac{s\,(a_s+2p_{\rm coex}l)}{T}\right] \text{ and } \rho_{\rm coex} = \sum_{s,A} A g_{s,A}\exp\left[-\frac{s\,(a_s+2p_{\rm coex}l)}{T}\right]. \tag{31}$$

were solved iteratively using $a_s = 2$ and the directly counted $g_{s,A}$ [126]. As one might expect, at low temperatures, where the dilute phase is very dilute, the "ideal" expressions of Eqs. (19) and (13) work quite well. However as the temperature increases and more and more clusters appear in the dilute phase the "ideal" expressions fail and predict, as expected based on the cluster concentration predictions, pressure and density values that are higher than the Onsager solution. The finite volume expressions of Eqs. (19) and (29) follow Onsager's solution and the Ising calculations more closely. The conclusion of this exercise is that a $\sim 10\%$ change in T_c from the "ideal" estimate is enough to approximately offset any effects of the finite volume of the clusters. Thus by leaving T_c as a free parameter when fitting cluster concentrations, or by obtaining T_c from other methods, one escapes, for the most part, any problems that arise from the finite volume of the clusters.

Summary

We have seen that Fisher's model is a physical cluster model. Fisher's main contribution was to introduce an accurate approximation for the entropic contribution to the cluster partition function. This lead to the development of a model that shows both types of scaling: the singular behavior of quantities near that critical point and the scaling laws that relate exponents as well as the data collapse of cluster concentrations. Fisher's model has an unphysical surface tension above the critical temperature, however below T_c it serves as a good approximation that lends itself easily to a physical interpretation. Though Fisher's assumption about the mean surface of a cluster is crude (using a constant values for a_0 and σ ignores the temperature dependence of the mean surface of a given cluster size) and it explicitly ignores the finite volume of the clusters (though implicitly the finite volume is almost all accounted for by the proper choice of T_c) it has successfully: described cluster production in percolating systems and Ising systems (see above); reproduced the compressibility factor at the critical point (see above); predicted (within a few percent) the compressibility factor of real fluids from the triple point to the critical temperature [12, 52]; and has been used to describe the nucleation rate of real fluids [14, 42].

A BRIEF HISTORY OF EXPERIMENTAL NUCLEAR CLUSTER PRODUCTION

In the beginning there was neutron evaporation [1, 2], *and the evaporation was good* [4]...

It was noted long ago that statistical methods could be applied to nuclear processes if the energies involved are large when compared to the lowest excitation energies of nuclei [1]. By doing this, Weisskopf was able to formulate expressions for the probability of neutron (or charged particle) emission from excited nuclei. Weisskopf based his work on the formula for the probability of evaporation from a body at low temperatures. In that regard, Weisskopf was working out the formula to describe the evaporation of neutrons from a hot nucleus, i.e. he was describing a first order phase transition in nuclear matter with a neutron leaving the condensed phase (the hot nucleus) and entering the dilute phase (a very low density neutron vapor).

Following Bohr, Weisskopf divided processes initiated by nuclear collisions into two stages: the first was the formation of a compound nucleus and the second was the disintegration of the compound nucleus. Both stages could be treated independently. The energy of the compound nucleus is similar to the heat energy in a solid or liquid and the emission of particles from the compound nucleus is analogous to an evaporation process and Weisskopf derived a general statistical formula for the evaporation of particles from an excited compound nucleus (with the caveats of the finiteness of the nucleus and the fact that the evaporation of a particle takes away significant energy from the compound nucleus).

The probability per unit time of a nucleus A_0 with excitation energy E^* emitting a neutron of mass m with kinetic energy between $\mathscr{E}$ and $\mathscr{E}+d\mathscr{E}$ (where de is much larger than the levels of A_0), thus transforming itself into nucleus A_c with an excitation energy $E^*-E_0-\mathscr{E}$ (where E_0 is the neutron binding energy of A_0) is

$$W_n(\mathscr{E})\,d\mathscr{E}=\sigma(E_0,\mathscr{E})\,\frac{m\mathscr{E}}{\pi^2\hbar^3}\exp\left\{-\frac{\mathscr{E}-T\left[\ln g+S_A-S_B-f(\mathscr{E})\right]}{T}\right\}d\mathscr{E} \tag{32}$$

where $\sigma(E_0,e)$ is the mean cross section for the collision of a neutron of kinetic energy e with nucleus A_c of energy E^*-E_0-e resulting in the production of nucleus A_0 of energy E^*; g is the number of states for the spin of the particle under consideration; $S(E)=\ln\omega(E)$ corresponds to the entropy of a nucleus with and energy between E and $E+dE$ (and density of levels $\omega(E)$); T is the temperature at which E is the most probable energy of nucleus A_c; and $f(e)$ "contains all further terms of the development." The probability per unit time for the evaporation of particles of charge Z from nucleus A_0 is

$$W_P(\mathscr{E})\,d\mathscr{E}=\pi R_0^2\left(\mathscr{E}-e^2\frac{Z_0Z}{R_0}\right)\frac{m}{\pi^2\hbar^3}\exp\left\{-\frac{\mathscr{E}+e^2\frac{Z_0Z}{r}-T\left[\ln g+S_A-S_B-f(\mathscr{E}-e^2\frac{Z_0Z}{R_0})\right]}{T}\right\}d\mathscr{E} \tag{33}$$

where R_0 is the radius of the compound nucleus and Z_0 is its charge. It is no surprise, given that Weisskopf had evaporation in mind, that equations (32) and (33) are similar to Fisher's estimate of the cluster partition function given in Eq. (9).

Multiplying the total probability of particle emission by $\hbar$ then gives the decay width: for neutrons:

$$\Gamma_n=\overline{\sigma}\frac{m}{\pi^2\hbar^2}T^2\exp\left(\ln g+S_A-S_B\right) \tag{34}$$

(where $\overline{\sigma}$ is the mean value of $\sigma(E_0,\mathscr{E})\,f(\mathscr{E})$ averaged over the Maxwell distribution) and for charged particles

$$\Gamma_P=\sigma_0\frac{m}{\pi^2\hbar^2}T^2\exp\left(\ln g+S_A-S_B\right). \tag{35}$$

Thus Weisskopf developed a theory of nuclear evaporation, i.e. a theory of first order phase transition in finite, charged, asymmetric nuclear matter.

Experimental evidence of neutron evaporation appeared in the energy distributions of neutrons measured after various nuclei were bombarded with 190 MeV protons [4]. Equation (32) gives the probability of the evaporation of a single neutron from a single compound nucleus at a specific excitation energy. However, experimental measurements of neutron kinetic energy distributions were measured for neutrons that came from a cascade of successive evaporations from compound nuclei with a distribution of initial excitation energies. Thus to connect Eq. (32) with the experimental

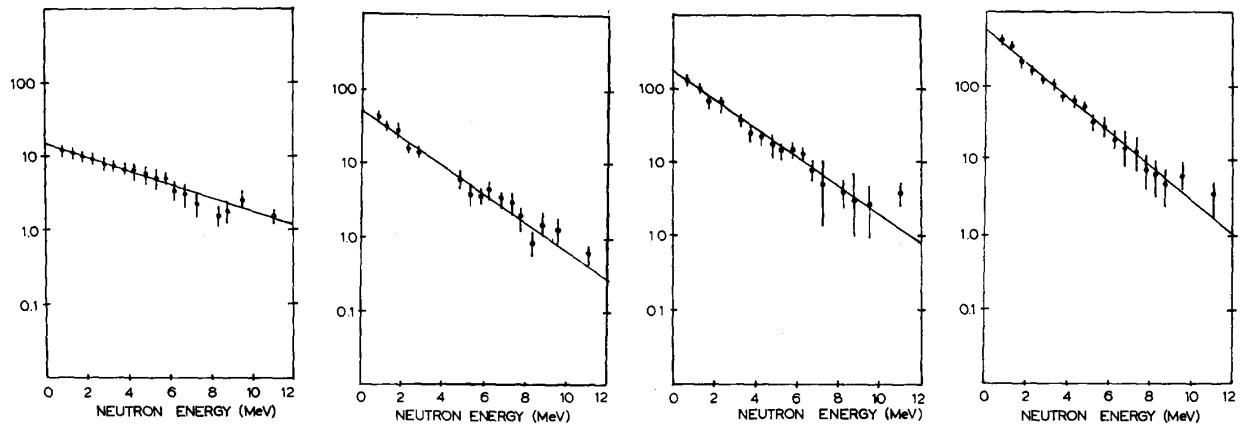

FIGURE 8. The scaled energy distributions of neutrons ($\frac{W_n(\mathscr{E})}{\sigma(E_0,\mathscr{E})\mathscr{E}^{1-i}}$ vs. $\mathscr{E}$) evaporated from (left to right): Al, Ni, Ag and Au nuclei after bombardment from 190 MeV protons [4]. The slopes of the lines give the inverse of the effective temperature of evaporation.

measurements the successive neutron (and proton) evaporation and distributions of initial excitation energies had to be taken into account which gives [4]

$$W_n(\mathscr{E})\,d\mathscr{E} \propto \sigma(E_0,\mathscr{E})\left(\frac{\mathscr{E}}{T}\right)^{i-1}\exp\left(-\frac{\mathscr{E}}{T}\right)\frac{1}{T}d\mathscr{E} \tag{36}$$

where i is the generation of the evaporation. Figure 8 shows logarithmic plots of scaled neutron energy distributions ($\frac{W_n(\mathscr{E})}{\sigma(E_0,\mathscr{E})\mathscr{E}^{1-i}}$ vs. $\mathscr{E}$) follow a straight line whose slope is the inverse of the effective temperature of evaporation T. The plots in Fig. 8 are similar to the Arrhenius plots of nuclear cluster yields observed much latter [72], as such they present early evidence for thermal scaling in nuclear evaporation.

If the analogous behavior of evaporation from excited nuclei and evaporation of classical fluids holds, then one expects that as the temperature increases the first order phase transition (evaporation) becomes a continuous phase transition at a critical temperature T_c above which there is a smooth cross over from the condensed phase to the dilute phase. Thus, when inclusive cluster yields from the reaction of $80 \leq E_{\text{beam}} \leq 350$ GeV protons incident on krypton and xenon nuclei exhibited a power law (as expected for $n_A(T_c)$ in Eq. (13)) with an exponent between 2 and 3 (as expected for $d = 3$ systems [20]) it seemed possible that the critical temperature had been reached [24, 26, 27].

REFERENCES

1. V. Weisskopf, Phys. Rev. **52**, 295 (1937).
2. H. A. Bethe, Rev. Mod. Phys. **9**, 69 (1937).
3. E. A. Guggenheim, J. Chem. Phys., **13**, 253 (1945).
4. K. J. Le Couteur and D. W. Lang, Nucl. Phys. **13**, 32 (1959).
5. M. E. Fisher, Phys. Rev. Lett. **16**, 11 (1966).
6. M. S. Green *et al*., Phys. Rev. Lett. **18**, 1113 (1967).
7. M. E. Fisher, Physics (N.Y.) **3**, 255 (1967).
8. M. E. Fisher, Rep. Prog. Phys. **30**, 615 (1967).
9. C. S. Kiang, Phys. Rev. Lett. **24**, 47 (1970).
10. C. S. Kiang and D. Stauffer, Z. Phys. **235**, 130 (1970).
11. D. Stauffer and C. S. Kiang, Phys. Rev. Lett. **27**, 1783 (1971).
12. W. Rathjen *et al*., Phys. Lett. **40A**, 345 (1972).
13. E. Stoll *et al*., Phys. Rev. B **6**, 2777 (1972).
14. D. Stauffer *et al*., Phys. Rev. B **6**, 2780 (1972).
15. K. Binder and H. Müller-Krumbhaar, Phys. Rev. B **9**, 2328 (1974).
16. D. Landau, Phys. Rev. B **13**., 2997 (1976).
17. D. Landau, Phys. Rev. B **14**., 255 (1976).
18. D. Stauffer and C. S. Kiang, Adv. Coll. Intr. Sci. **7**., 103 (1977).

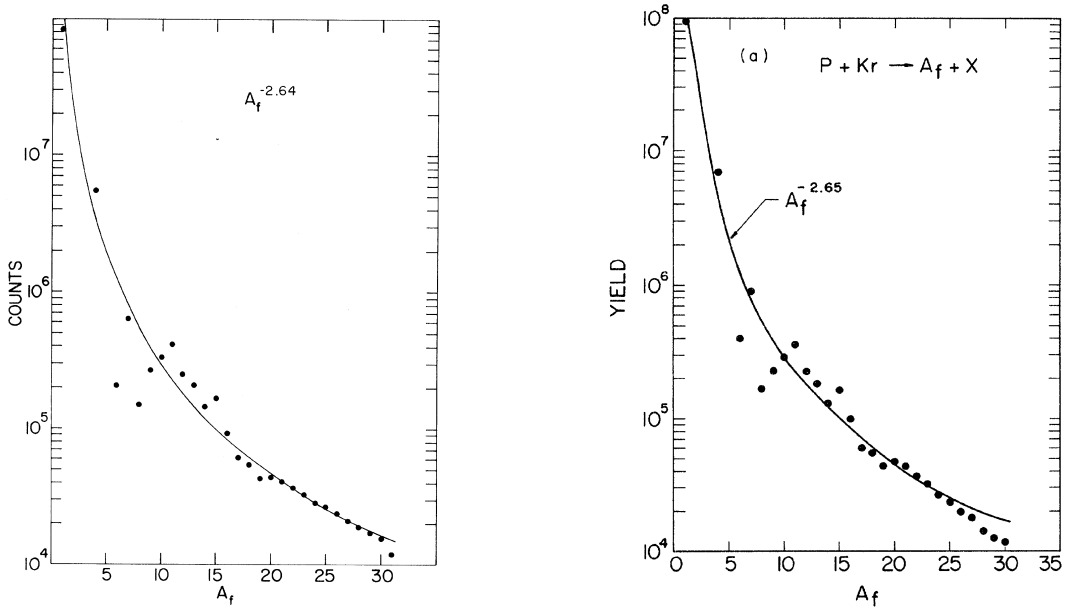

FIGURE 9. The inclusive cluster yields n_A as a function of cluster size A from the reaction of $80 \leq E_{\text{beam}} \leq 350$ GeV protons incident on xenon (left [24]) and krypton (right [27]) nuclei. Solid lines show a fit to the data with a power law.

19. A. Levelt Sengers *et al*., Phys. Tod., 42 (1977).
20. D. Stauffer, Phys. Rep. **54**, 1 (1979).
21. A. Coniglio and W. Klein, J. Phys. A **13**, 2775 (1980).
22. H. Nakanishi and H. E. Stanley, Phys. Rev. B, **22**, 2466 (1980).
23. J. L. Lebowitz and E. M. Waisman, Phys. Tod., 24 (1980).
24. J. E. Finn *et al*., Phys. Rev. Lett. **49**, 1321 (1982).
25. H. Jaqaman *et al*., Phys. Rev. C **27**, 2782 (1983).
26. P. J. Siemens, Nature **305**., 410 (1983).
27. A. S. Hirsch *et al*., Phys. Rev. C **29**, 508 (1984).
28. A. Margolina *et al*., J. Phys. A **17**, 1683 (1984).
29. A. Perini *et al*., Phys. Rev. B **29**, 2689 (1984).
30. H. Jaqaman *et al*., Phys. Rev. C **29**, 2067 (1984).
31. A. L. Goodman *et al*., Phys. Rev. C **30**, 851 (1984).
32. W. Bauer *et al*., Phys. Lett. **150B**, 53 (1985).
33. P. Bonche *et al*., Nucl. Phys. A **436**, 265 (1985).
34. S. Levit *et al*., Nucle. Phys. A **437**, 426 (1985).
35. X. Campi, J. Phys. A **19**, L917 (1986).
36. J. L. Cambier and M. Nauenberg, Phys. Rev. B **34**, 8071 (1986).
37. M. Mahi *et al*., Phys. Rev. Lett. **60**, 1936 (1988).
38. X. Campi, Phys. Lett. B **208**, 351 (1988).
39. W. Bauer, Phys. Rev. C **38**, 1297 (1988).
40. J. S. Wang, Physica A **161**, 249 (1989).
41. S. Redner, *Statistical models for the fracture of disordered media*, H. J. Herrmann and S. Roux eds., Elsevier, North-Holland, 321 (1990).
42. A. Dillmann and G. E. A. Meier, J. Chem. Phys. **94**, 3872 (1990).
43. A. M. Ferrenberg and D. P. Landau, Phys. Rev. B **44**, 5081 (1991).
44. C. A. Ogilvie *et al*., Phys. Rev. Lett. **67**., 1214 (1991).
45. L. Phair *et al*., Phys. Lett. B **285**, 10 (1992).
46. L. Phair *et al*., Phys. Lett. B **314**, 271 (1993).
47. L. G. Moretto *et al*., Phys. Rev. Lett. **71**, 3935, (1993).
48. J. B. Elliott *et al*., Phys. Rev. C **49**, 3185 (1994).
49. C. O. Dorso and P. E. Balonga, Phys. Rev. C **50**, 991 (1994).
50. M. L. Gilkes *et al*., Phys. Rev. Lett. **73**, 1590 (1994).
51. V. Latora *et al*., Phys. Rev. Lett. **73**, 1765 (1994).
52. D. Saltz, J. Chem. Phys. **101**, 6038 (1994).

53. L. G. Moretto *et al*., Phys. Rev. Lett. **74**, 1530 (1995).
54. L. Phair *et al*., Phys. Rev. Lett. **75**, 213 (1995).
55. M. Belkecam *et al*., Phys. Rev. C **52**, 271 (1995).
56. H. Müller and B. D. Serot, Phys. Rev. C **52**, 2072 (1995).
57. K. Tso *et al*., Phys. Lett. B **361**, 25 (1990).
58. J. J. Alonso *et al*., Phys. Rev. E **52**, 6006 (1995).
59. P. Finocchiaro *et al*., Nucl. Phys. A **600**, 236 (1996).
60. S. Das Gupta and J. Pan, Phys. Rev. C **53**, 1319 (1996).
61. J. B. Elliott *et al*., Phys. Lett. B **381**, 35 (1996).
62. C. O. Dorso and A. Strachan, Phys. Rev. B **54**, 236 (1996).
63. W. F. J. Müller *et al*., *Proceedings of the Catania Relativistic Ion Studies, Acicastello, May 1996*, World Scientific (1996).
64. L. Phair *et al*., Phys. Rev. Lett. **77**, 822 (1996).
65. S. Das Gupta *et al*., Phys. Rev. C **54**, 2820 (1996).
66. M. Belkacem *et al*., Phys. Rev. C **54**, 2435 (1996).
67. X. Campi and H. Krivine, Nucl. Phys. A **620**, 46 (1997).
68. A. Strachan and C. O. Dorso, Phys. Rev. C **55**, 775 (1997).
69. J. B. Elliott *et al*., Phys. Rev. C **55**, 1319 (1997).
70. V. N. Kondratyev *et al*., J. Chem. Phys. **106**, 7766 (1997).
71. I. J. Ford, J. Chem. Phys. **106**, 9734 (1997).
72. L. G. Moretto *et al*., Phys. Rep. **287**, 249 (1997).
73. W. F. J. Müller, Phys. Rev. C **56**, 2873 (1997).
74. J. B. Elliott *et al*., Phys. Lett. B **418**, 34 (1998).
75. M. B. Tsang and P. Danielewicz, Phys. Rev. Lett. **80**, 1178 (1998).
76. L. G. Moretto *et al*., LBNL-42617 (1998).
77. J. Pan *et al*., Phys. Rev. Lett. **80**, 1182 (1998).
78. J. Pan and S. Das Gupta, Phys. Rev. C **57**, 1839 (1998).
79. L. Beaulieu *et al*., Phys. Rev. Lett. **81**, 770 (1998).
80. A. Strachan and C. O. Dorso, Phys. Rev. C **58**, R632 (1998).
81. J. Richert *et al*., Nucl. Phys. A **639**, 717 (1998).
82. J. M. Carmona *et al*., Nucl. Phys. A **643**, 115 (1998).
83. J. S. Sá Martins and P. M. C. de Oliveria, Nucl. Phys. A **643**, 433 (1998).
84. H. E. Stanley, Rev. Mod. Phys. **71** S358 (1999).
85. A. Strachan and C. O. Dorso, Phys. Rev. C **59**, 285 (1999).
86. F. Gulminelli and Ph. Chomaz, Phys. Rev. Lett. **82**, 1402 (1999).
87. M. D'Agostino *et al*., Nucl. Phys. A **650**, 329 (1999).
88. W. Bauer and S. Pratt, Phys. Rev. C **59**, 2695 (1999).
89. I. Jensen and A. J. Guttmann, J. Phys. A **32**, 4867 (1999)
90. S. K. Samaddar *et al*., Phys. Lett. B **459**, 8 (1999).
91. Y. G. Ma *et al*., Phys. Rev. C **60**, 024607 (1999)
92. L. G. Moretto *et al*., Phys. Rev. C **60**, 031601 (1999).
93. C. O. Dorso *et al*., Phys. Rev. C **60**, 034606 (1999).
94. X. Campi *et al*., Eur. Phys. J. D **11**, 233 (2000).
95. W. Janke and R. Villanova, Nucl. Phys. B **83**, 697 (2000).
96. J. M. Carmona *et al*., Phys. Rev. C **61**, 037304 (2000).
97. L. G. Moretto *et al*., Phys. Lett. B **484**, 192 (2000).
98. L. Beaulieu, Phys. Rev. Lett. **84**, 5971 (2000).
99. T. S. Fan *et al*., Nucl. Phys. A **679**, 121 (2000).
100. H. S. Xu *et al*., Phys. Rev. Lett. **85**, 716 (2000).
101. J. B. Elliott *et al*., Phys. Rev. Lett. **85**, 1194 (2000).
102. J. Richert and P. Wagner, Phys. Rep. **350**, 1 (2001).
103. Y. G. Ma, arXiv:nucl-th/0010063 (2000).
104. J. B. Elliott *et al*., Phys. Rev. C **62**, 064603 (2000).
105. L. Beaulieu *et al*., Phys. Rev. C **63**, 031302 (2001).
106. S. M. Bhattacharjee and F. Seno, J. Phys. A **34**, 6375 (2001).
107. X. Campi *et al*., Nucl. Phys. A **681**, 458c (2001).
108. J. M. Carmona *et al*., Eur. Phys. J. A **11**, 87 (2001).
109. M. B. Tsang *et al*., Phys. Rev. Lett. **86**, 5023 (2001).
110. C. B. Das and S. Das Gupta, Phys. Rev. C **64**, 017601 (2001).
111. M. B. Tsang *et al*., Phys. Rev. C **64**, 041603 (2001).
112. M. B. Tsang *et al*., Phys. Rev. C **64**, 054615 (2001).
113. L. Beaulieu *et al*., Phys. Rev. C **64**, 064604 (2001).
114. M. N. Andronenko *et al*., arXiv:nucl-ex/0112014, PNPI-2001-2458 (2001).
115. Y. G. Ma, J. Phys. G **27**, 2455 (2001).

116. M. Kleine Berkenbusch *et al*., Phys. Rev. Lett. **88**, 022701 (2002).
117. J. B. Elliott *et al*., Phys. Rev. Lett. **88**, 042701 (2002).
118. J. M. Carmona *et al*., Phys. Lett. B **531**, 71 (2002).
119. C. B. Das *et al*., Phys. Rev. C **65**, 034608 (2002).
120. Y. G. Ma, arXiv:nucl-th/0203065 (2002).
121. F. Gulminelli *et al*., Phys. Rev. C **65**, 051601 (2002).
122. D. Cussol, Phys. Rev. C **65**, 054615 (2002).
123. A. Chernomoretz *et al*., arXiv:nucl-th/0203050 (2002).
124. P. Balenzuela *et al*., Phys. Rev. C **66**, 024613 (2002).
125. C. B. Das *et al*., Phys. Rev. C **66**, 044602 (2002).
126. I. Jensen, private communication (2003).
127. N. Sator, Phys. Rep, **376**, 1 (2003).
128. X. Campi *et al*., Phys. Rev. C **67**, 044610 (2003).
129. M. D'Agostino *et al*., Nucl. Phys. A **724**, 455 (2003).
130. J. B. Elliott *et al*., Phys. Rev. C **67**, 024609 (2003).
131. J. Engels *et al*., Nucl. Phys. B **655**, 277 (2003).
132. G. A. Souliotis *et al*., Phys. Rev. C **68**, 024605 (2003).
133. W. P. Tan *et al*., arXiv:nucl-ex/0311001 (2003).
134. D. V. Shetty *et al*., Phys. Rev. C **68**, 054605 (2003).
135. C. M. Mader *et al*., Phys. Rev. C **68**, 064601 (2003).
136. J. B. Elliott *et al*., LBNL NSD Ann. Rep. (2003).
137. J. B. Elliott *et al*., LBNL NSD Ann. Rep. (2003).
138. J. B. Elliott *et al*., LBNL NSD Ann. Rep. (2003).
139. J. B. Elliott *et al*., LBNL NSD Ann. Rep. (2003).
140. J. Helgesson and R. Ghetti, private communication (2004).
141. M. D'Agostino *et al*., Nucl.Phys. A **734**, 512 (2004).
142. W. A. Friedman, Phys. Rev. C **69**, 031601 (2004).
143. M. Veselesky *et al*., Phys. Rev. C **69**, 031602 (2004).
144. S. R. Souza *et al*., Phys. Rev. C **69**, 031607 (2004).
145. D. V. Shetty *et al*., Phys. Rev. C **70**, 011601 (2004).
146. M. F. Rivet *et al*., Nucl.Phys. A **749**, 73 (2005).
147. J. B. Elliott *et al*., Phys. Rev. C **71**, 024607 (2005).
148. L. G. Moretto *et al*., Phys. Rev. Lett. **94**, 202701 (2005).
149. L. G. Moretto *et al*., arXiv:nucl-ex/0507015, LBNL-58153 (2005).